

Interplay of Oct4 with Sox2 and Sox17: a molecular switch from stem cell pluripotency to specifying a cardiac fate.

Sonia Stefanovic, Nesrine Abboud, Stéphanie Désilets, David Nu, Chad Cowan, Michel Puceat

▶ **To cite this version:**

Sonia Stefanovic, Nesrine Abboud, Stéphanie Désilets, David Nu, Chad Cowan, et al.. Interplay of Oct4 with Sox2 and Sox17: a molecular switch from stem cell pluripotency to specifying a cardiac fate.. Journal of Cell Biology, 2009, 186 (5), pp.665-73. 10.1083/jcb.200901040 . inserm-00409113

HAL Id: inserm-00409113

https://inserm.hal.science/inserm-00409113

Submitted on 10 Sep 2009

HAL is a multi-disciplinary open access archive for the deposit and dissemination of scientific research documents, whether they are published or not. The documents may come from teaching and research institutions in France or abroad, or from public or private research centers.

L'archive ouverte pluridisciplinaire **HAL**, est destinée au dépôt et à la diffusion de documents scientifiques de niveau recherche, publiés ou non, émanant des établissements d'enseignement et de recherche français ou étrangers, des laboratoires publics ou privés.

JCB MS# 200901040R2

Interplay of Oct4 with Sox2 and Sox17: a molecular switch from stem cell pluripotency to specifying a cardiac fate

Sonia Stefanovic[1], Nesrine Abboud[1]*, Stéphanie Désilets[1]*, David Nury[1], Chad Cowan[2], Michel Pucéat[1,§]

[1]INSERM -Avenir Team, *stem cells and cardiogenesis,* Evry, France

[2]Stowers Medical Institute, Center for Regenerative Medicine and Technology, Cardiovascular Research Center, Boston, USA

* equally contributed to this work

[§] to whom correspondence should be addressed:
INSERM/Avenir Team
Genopole Campus 1
4, rue Pierre Fontaine, 91058 Evry, France
michel.puceat@inserm.fr

abstract+introduction+results = 17534 +figureLegends 3035= 20569 characters

Oct4 exerts a dose-dependent dual action, as both a gatekeeper for stem cell pluripotency and in driving cells toward specific lineages. Here, we identify the molecular mechanism underlying this dual function. BMP2- or transgene-induced Oct4 up-regulation drives human embryonic and induced pluripotent stem cells to become cardiac progenitors. When ESC pluripotency is achieved, Oct4 switches from the *Sox2* to the *Sox17* promoter. This switch allows the cells to turn off the pluripotency Oct4-Sox2 loop and to turn on the *Sox17* promoter. This powerful process generates a subset of endoderm expressing *Sox17* and *Hex*, both regulators of paracrine signals for cardiogenesis (i.e., Wnt, BMP2) released into the medium surrounding colonies of ES cells. Our data thus reveals a novel molecular Oct4 and Sox17-mediated mechanism which disrupts the stem cell microenvironment favoring pluripotency to provide a novel paracrine endodermal environment in which cell lineage is determined and commits the cells to a cardiogenic fate.

.

Introduction

Embryonic stem cells (ESC), derived from the ICM of the blastocyst or induced pluripotent stem cells (iPSC) derived from reprogrammed somatic cells retain the ability to self-renew in culture and the potential to differentiate into any cell lineage. The ESC specific protein, Oct4, is one of the most ancient TF and is expressed very early during embryonic development (Smith, 1991). In mouse ESC, together with Sox2 and Nanog, Oct4 cooperatively maintains pluripotency through a tightly regulated transcriptional loop (Loh et al., 2006; Niwa, 2007). However, a new function of this TF has recently emerged in the process of cell lineage determination. In fact, the level of Oct4 in ESC determines its dual function (Niwa et al., 2000). The mechanism of that process remained unknown. We demonstrated *in vitro* and *in vivo* a gene dosage-dependent function of Oct4, driving ESC or the epiblast toward a mesodermal cardiogenic fate (Zeineddine et al., 2006).

However, the genetic and epigenetic mechanisms underlying the dual function of Oct4, maintaining pluripotency or inducing lineage progression, has remained puzzling. Furthermore, whether this concept applies to human pluripotent cells is also questionable.

Results and discussion

We chose the cardiac lineage, determined as early as within the epiblast (Tam PPL and Schoenwolf, 1999) to analyse the dual function of Oct4. First, we tested whether BMP2-induced cardiac commitment and differentiation of HESC (Tomescot et al., 2007) was associated with modulation of Oct4. Expression of both human Oct4 isoforms, Oct4-iA, maintaining cell pluripotency (Lee et al., 2006), and Oct4-iB of still unknown function, was monitored by RT-Q-PCR. Oct4-iA was up-regulated 3 fold in response to BMP2 . Expression of Oct4-iB remained unchanged (Fig.1A). We then used a HESC line harbouring a reporter gene (HUES-9 pOct4/GFP, Oct4*p* driving EGFP) (Inset Fig. 1B) to investigate BMP2-

mediated regulation of the Oct4*p*. First, to ensure that *GFP* was under the tight control of the Oct-4*p* , the HUES-9 pOct4/GFP cell line was nucleofected with COUP-TFI, a repressor of Oct4 (Ben-Shushan et al., 1995). GFP was switched-off in cells expressing COUP-TFI as shown by poor GFP distribution within colonies when compared to a fully green mock colony (Fig. S1A). Furthermore, over-expression of Oct4-iA in HUES-9 pOct4/GFP line increased GFP expression as expected from regulation of *Oct4p* by its own protein (Fig. S1B). Stimulation of this line with BMP2 up-regulated *GFP* mRNAs (Fig.1B) and FACS revealed a 70% increase in the highly positive GFP population (Fig. 1C).

To investigate whether a rise in Oct4-iA induces loss in cell pluripotency and promotes cell lineage specification, HESC were nucleofected with *Oct4-iA*, or *EGFP* cDNA (mock cells). Cells were cultured for 4d with FGF2. *Oct4-iA*-OEC (35 times), -2 fold more protein (inset 1E)-, did not change expression of Oct4-iB (Fig. 1E). Indeed only the 48kD (Oct4-iA), but not the 35kD band (Oct4-iB), was increased (inset 1E). SSEA-1 was first used as an early marker of HESC loss of pluripotency (Hoffman and Carpenter, 2005). Less than 1% mock cells (EGFP nucleofected) while 68% of Oct4-nucleofected cells expressed SSEA-1 (Fig. 1D). This percentage (68%), normalised to the one of cell nucleofection assessed by scoring GFP^+ cells (42%) (inset Fig. 1D) suggests that Oct4-iA-OEC as well as neighbouring cells had entered a differentiation program. To examine which lineage was induced by Oct4, gene expression was monitored by Q-PCR. Oct4-iA-OEC expressed both mesodermal (*Brachyury, Tbx6*) and cardiac (*Mesp1/2, Tbx20, Tbx5, Mef2C, Nkx2.5, cardiac* α*-Actin*) markers (Fig. 1E). Endodermal genes *Hex* and *Sox17* were also switched on by Oct4-iA (Fig. 1F). Furthermore, the corresponding proteins Sox17, Nkx2.5 and Mef2c were present HCC imaging assay allowed us to monitor more than 2500 cells and revealed that 48% of cells expressed Sox17, indicating that all nucleofected cells expressed the protein (when normalised to % of Oct4-iA nucleofection 42%, Fig. 1D). Up to 20% (i,e 48% of nucleofected cells) expressed Mef2c and

31% (74 % of nucleofected cells) Nkx2.5 (Fig. 1G). Very low expressions of the hematopoietic CD45, of the endothelial CD31, CD34 markers were detected (Fig. S1C). Thus, PCR, IF, and FACS data demonstrate that up-regulation of Oct4iA forces HESC to exit pluripotency to adopt a cardiovascular fate. Furthermore, the cardiogenic action of Oct4-iA was translated into a full cardiac differentiation program. While mock-nucleofected cells gave rise to cardiomyocytes expressing actinin- and cTnT, the later proteins were not yet organised in sarcomeric units 4 weeks after EBs formation. In contrast EBs generated from Oct4-iA-OEC featured 3.1 ± 0.2 (n=4) as many $cTnT^+$ and $actinin^+$ myocytes as in mock EBs, as assessed by measuring the anti-cTnT and –actinin fluorescent areas within whole EBs. Furthermore, the cardiomyocytes were assembled in strands and featured organised and adult-size sarcomeres (2 μm) (Fig. 1 H).

Next, we hypothesized that, to trigger specification to a cell lineage, increased Oct4 should disrupt the Sox2/Oct4 pluripotency loop. A potential candidate, to replace Sox2 as an Oct4 target, namely Sox17, recently reported as essential for early cardiogenesis (Liu et al., 2007) was expressed in Oct4-iA-OEC (Fig.1FG). We therefore tested the presence of Oct4 on Sox17*p*. ChIP assays designed to pull down Oct4-bound chromatin revealed that BMP2 led to 10 fold decrease in enrichment of DNA fragments containing the *Sox2* distal enhancer (Chew et al., 2005) and a 300 fold increase in the enrichment of DNA fragments containing a region of the *Sox17p* within the 700 bp upstream the transcription start site (Fig. 2AB). This result obtained in HUES-24 line was confirmed in 2 other HESC lines (H9.2 and I4). This was accompanied with induction of *Sox17* in BMP2-treated cells (right inset B). Oct4-iA-OEC featured a loss in Oct4-iA binding *Sox2* DNA including the distal enhancer and a gain in binding *Sox17p* (Fig. 2CD). In line with these data, ChIP from Oct4-iA-OEC using anti-modified-H3 antibodies revealed significant changes in methylation and acetylation of H3 associated with both *Sox2* and *Sox17* enhancer and promoter, respectively when compared to

mock cells (i.e. GFP nucleofected). While the ratio of methylations of K4 *vs* that of K27 of H3, as well as acetylation of H3K9 associated with *Sox2* distal enhancer was decreased, these were increased for the *Sox17p*. This pointed to repression of *Sox2* and activation of *Sox17p*, respectively (Fig. 2E). Furthermore, the Oct4/Sox2 interaction in control was lost upon up-regulation of Oct4-iA (Fig. 2F).

These transcriptional and epigenetic events led to Sox17 expression in BMP2-stimulated HUESC (Fig. 2G). A similar effect was observed in Oct4-iA-OEC (Fig. 1G). To gain more insight into the molecular mechanism of the switch of Oct4-iA from the *Sox2p* to the *Sox17p* we manipulated the level of expression of Sox2 in Oct4-iA-OEC, surmising that a stoichiometric competition occurs between Sox2 and Sox17. A displacement of Oct4/Sox2 complex on *Sox2* distal enhancer would permit Oct4 binding to *Sox17p*, turning on the gene and the protein, which would reinforce *Sox17* expression by forming an Oct4/Sox17 complex on its promoter.

When Sox2 was up-regulated in cells nucleofected with the cDNA (Fig. S1D), the gain in enrichment of Oct4-iA on the *Sox17p* was lost. When Sox2 was down-regulated using a ShRNA (Chew et al., 2005) (Fig. S1DE), Oct4-iA binding to the *Sox17p* was dramatically increased (Fig. 2H). We next looked for Oct4-Sox17 interaction in END-2 cells, an endodermal cell line expressing Sox17 (Mummery et al., 1991). Using co-IP after over-expression of Oct4-iA in this cell line, we found that Sox17 binds Oct4 (Fig. 2I). Altogether, our findings point to Sox17, a novel target of Oct4 also interacting with it, to compete with Sox2 to switch HESC from a pluripotent toward an endodermal/mesodermal fate.

To clarify whether Sox17 accounts for the switch of HESC from pluripotency to mesodermal and cardiac commitment of ESC, we used a ShRNA approach. *Sox17* ShRNA was nucleofected in HESC together with Oct4-iA cDNA. *Sox17* mRNA was then reduced in the presence of an increased level of Oct4. The protein was also 3 times less induced by Oct4

over-expression (Fig. S1F). The amount of Sox17 upon Oct4-iA up-regulation was thus too limited to significantly trigger cardiogenesis (Fig. 3A). Similarly, BMP2, which induces *Sox17* together with mesodermal and cardiac genes, could no longer induce these genes in the presence of *Sox17* ShRNA (Fig. S1G).

However, Sox17 ShRNA did not prevent the loss of *Sox2* DNA elements bound to Oct4-iA when over-expressed. Interestingly, under the same condition (i.e. Sox17 silencing), the *Sox17p* was no longer occupied by Oct4-iA (Fig. 3B). Thus, taken together, these ChIP experiments (Fig. 2&3) showed the occupancy of *Sox17p* by Oct4. They further revealed a predominance of K4 over K27 methylations, and an increase in K9 acetylation on H3 in the vicinity of the promoter, thus favouring an active chromatin state. This leads to gene and protein expression. The opposite scenario occurs on the *Sox2* distal enhancer (loss of Oct4 occupancy of the enhancer, increase in K27 methylation and a decrease in K9 acetylation of H3). Manipulating the levels of Sox2 and Sox17 further pointed to a competition between both Soxs as shown by the capability of Oct4 to form a complex with Sox17. We can further surmise that Oct4/Sox2 ratio is instrumental in creating various complexes with specific Sox proteins and/or DNA elements. At a normal level of Oct4 or Oct4/Sox2 ratio, it targets the Oct4-Sox2 enhancer, maintaining the transcriptional Oct4/Sox2/Nanog loop and thus cell pluripotency. At a higher Oct4 level or at a low level of Sox2, the POU factor targets the *Sox17p* triggering expression of the protein, forming a more stabilised Oct4/Sox17 complex on the *Sox17p*. This mechanism drives the cells toward specific endo/mesodermal fates.

Sox17 is known to target genes encoding cardiogenic factors such as Wnts (Zorn et al., 1999). Wnt is also a trigger of BMP2 (Kasai et al., 2005). To test whether Oct4-iA and Sox17 operate in a cell non autonomous manner, the conditioned medium (CM) from *Oct4-iA*-OEC was collected to test its potential to induce cardiogenesis. CM from Oct4-iA-OEC, triggers in *wt* HESC, expression of *Brachyury*, *Mesp1/2, Tbx20, Tbx5, Tbx6, Nkx2.5*, and *cardiac α-*

actin, as well as *Oct4-iA* (. 4A). CM from cells over-expressing *GFP* used as a control did not show any gene induction. Furthermore, CM from Oct4-iA-OEC applied to *wt* cells triggered a switch of Oct4-iA binding from the *Sox2* distal enhancer to the *Sox17p* (Fig. 4B). We also mixed in the same well HUES-9 pOct4/GFP cells nucleofected with Oct4-iA cDNA with mock cells at different ratios (0:1; 1:1; 3:1; 9:1, respectively). After 4 d of coculture, mock cell colonies were dissected out and used in real time PCR. Expression of *Tbx6 Mesp1, Isl1, Nkx2.5, Tbx5* was significantly induced in mock cells when they were mixed with at least 3 times as many Oct4-iA-OE HUES-9 pOct4/GFP cells as mock cells (3:1 ratio) (Fig. S2A). In another set of experiments, mixed cells were fixed and stained with an anti-Nkx2.5 antibody. These experiments showed that $Nkx2.5^{+}$ cells were mainly mock HUESC neighbouring GFP^{+} cells (Fig. S2B) further confirming that Oct4-iA-OEC exert their cardiogenic function through secretion of cardiogenic factors.

We hypothesized that BMP2 or/and Wnt, both direct or indirect targets of Sox17/Hex pathway, as well as Nodal, a Sox17 inducer, might be cardiogenic candidates released by OctiA- and Sox17-OEC. Thus, HESC were nucleofected with *Oct4-iA* cDNA and then cultured for 4 d in the absence or in the presence of 150 ng/ml Dipkopf (DKK), 100 ng/ml Noggin or 10 ng/ml Lefty to prevent Wnt, BMP2 or Nodal signalling, respectively. Figure 4C shows that both DKK and Noggin but not Lefty prevented Oct4-iA-induced expression of *Brachyury, Mesp, Tbx20, Tbx5, Tbx6 and Nkx2.5*. Challenging HESC with BMP2 (10 ng/ml) together with Wnt3a (50 ng/ml) significantly improved the effect of BMP2 on early cardiac gene expression as well as on BMP2 and Wnt3a expression (Fig. S2C). In line with these data, Oct4-iA-OEC expressed *BMP2* and *Wnt3a* (Fig. 4D). Thus, BMP2 and Wnt3a are the cardiogenic factors released by Oct4 induced $Sox17^{+}$ cells. Four other findings confirmed this claim. First, phosphorylated smad recognized by an anti-phosphosmad 1,5,8 antibody was barely detectable in mock cells cultured alone but observed into nuclei of Oct4-iA-OEC in

wells including 50% (i.e., nucleofection efficiency) of *Oct4-iA*-OEC and 50% of non nucleofected cells (Fig. S3B). Second, anti-smad 4 ChIP experiments revealed a binding of smad to both the Nkx2.5 and Tbx6 promoters, 2 targets of BMP2 (Fig. S3A) in Oct4-iA-OEC. Third, Wnt3a signalling pathway was activated in Oct4-iA-OEC as visualized by nuclear localisation of β-catenin in contrast to the membrane staining observed in mock cells (Fig. S3B). Finally, both anti-BMP2 and anti-Wnt3a antibodies added for 2 d in the medium of Oct4-iA-OEC prevented expression of genes marking the mesoderm (*Tbx6*), the cardiogenic mesoderm (*Mesp1*) and cardiac progenitors (*Tbx5*) (data not shown).

To further investigate whether cells expressing Sox17 exerted their cardiogenic action through an autocrine and/or paracrine mechanism, HUES-9-pOct4/GFP cells were plated in microwells and stimulated for 4 d with BMP2. Cells expressing GFP were stained for Sox17 and Mesp1/2, the earliest cardiac marker. Cells not challenged with BMP2 did not express Sox17 or Mesp1/2 (Fig. 4E upper panel). Cells challenged with BMP2 expressed both Sox17 and Mesp1/2. Careful observation of cells revealed that a few BMP2-stimulated cells expressed both Sox17 and Mesp1/2 while most of them expressed only Sox17 or Mesp1/2. This differential expression of Sox17 and Mesp1/2 was observed in the same or neighbouring cell colonies. To further quantify the phenomenon, we set up a High-Content imaging assay. 32 wells and 50 fields per well were scanned for expression of GFP, Sox17 and Mesp1/2. Cells expressing GFP, Sox17, Mesp1/2 alone or expressing 2 or 3 markers were separately scored. The Venn Diagram (Fig. 4F) first revealed that about 50% of cells responded to BMP2 as 44 % did not express Sox17 and/or Mesp1/2. Half of responder cells (33% of total) expressed Sox17 and the other half (26% of total cells) expressed Mesp1/2. The diagram clearly shows that most of cells expressed only Sox17, with many still highly GFP^{+} or only Mesp2 having lost GFP. A minority of the cells expressed Sox17 and Mesp1/2; almost no cell expressed the 3 markers. While 40-50% cells were nucleofected and over-expressed Oct4-iA

cells, 40-60% also expressed several markers including Mef2c and Nkx2.5, which together confer to the cells a cardiac fate (Fig. 1G), further pointing to a robust paracrine effect of the latter. These findings suggest that the dual function of Oct4 is mediated by a paracrine phenomenon mediated by both BMP2 and Wnt3a. This claim is supported by 3 series of experiments (i) first, inhibitors or blocking antibodies suggesting the presence in the medium of Sox17 expressing cells of both Wnt, known to be a target of Sox17 (Zorn et al., 1999) and BMP2 which cooperates with Wnt pathway (Crease et al., 1998; Sumi et al., 2008; Kasai et al., 2005), (ii) second, the BMP2 and Wnt signaling paythways were both activated in wells containing Oct4-iA-overexpressing cells as revealed by intranuclear localisation of both P-smad 1,5,8 and β–catenin in these cells together with the binding of smad 4 to the *Nkx2.5p* and *Tbx6p* (iii) and third, expression of *BMP2* and *Wnt3a* mRNAs by Oct4-OEC. Indeed, both Wnt and BMP2 are well known cardiogenic factors (Liu et al., 2007; Menard et al., 2004). Wnt exerts a cardiogenic action early on during embryogenesis to establish the primitive streak/mesendoderm and then BMP2 together with Wnt drive the cells towards the posterior primitive streak and mesoderm (Bakre et al., 2007; Sumi et al., 2008). Furthermore, Wnt in the absence of Activin does not promote the hematopoietic lineage (Nostro et al., 2008) as well as Sox17 prevents the development of ectoderm (Seguin et al., 2008). Then, BMP2 takes over the cardiogenic task, Wnt becoming a cardiogenic inhibitor (Naito et al., 2006). The cardiogenic factors released by Oct4-induced $Sox17^{+}$ cells may exert their action in an autocrine, and/or in a paracrine manner on neighbouring Sox17 negative cells driving them from an undifferentiated to a mesodermal cardiogenic fate. Using HCC imaging, to monitor expression of Sox17 and Mesp2 in BMP2-induced Oct4-iA-OEC revealed that one third of Oct4-iA-OEC expressed Sox17 as expected from a direct targeting of Sox17 by the POU factor, while many cells expressing Mesp2 did not express any longer Oct4 or Sox17. This observation argues more for a paracrine effect although we cannot exclude a kinetic effect,

cells going through a endo/mesendodermal stage ($Sox17^+$) and then to the cardiogenic mesoderm ($Mesp1/2^+$) turning off Sox17 in line with the inhibitory effect of Mesp1/2 on Sox17 (Bondue et al., 2008).

Our data thus revealed a novel Oct4/Sox17-mediated molecular mechanism which disrupts the microenvironment that favors cell pluripotency and prevents differentiation, to provide a novel paracrine environment more prone to commit the cells toward a cardiac lineage.

iPSC are derived from somatic cells reprogrammed using Oct4, Sox2, Nanog and Lin28 or Myc (Takahashi et al., 2007). We wondered whether manipulating Oct4-iA level in such cells could also drive them through the Sox2/Sox17 switch toward a cardiogenic fate. Thus, iPSC were nucleofected with *Oct4-iA* cDNA and both gene expression and *Sox17p* occupancy were monitored by Q-PCR. Figure S3C shows that 5d post-nucleofection, iPSC expressing 10 times more *Oct4-iA* mRNA than GFP nucleofected cells changed of morphology, displaying more flat and irregular colonies in comparison with compact colonies in mock cells expressing GFP. These cells expressed mesodermal and cardiac markers including *Brachyury, Mesp1/2, Tbx20, Tbx5*, and *Nkx2.5* as well as *Sox17* (Fig. S3D). Oct4-iA switched from the *Sox2* to the *Sox17p* (Fig. S3E). This was associated with up-regulation of *Sox17* (inset Fig. S3D) and of both *Wnt3a* and *BMP2* mRNAs (Fig. S3F).

Thus, we have found a novel molecular and cellular circuit in which Oct4 and Sox17 work in combination to drive human pluripotent stem cells toward an endodermal or mesendodermal fate, and in turn toward the fate of cardiac progenitors. This circuit is functional within a ESC colony or “niche”, BMP2 acting first in cells surrounding the colony, likely generating a gradient from the outer to the inner part of colonies rather secreting factors such as GDF3 maintaining a basal level of Oct4 and cell pluripotency (Peerani et al., 2007). Then, mesendo/endodermal $Sox17^+$ cells amplify the differentiation process by secreting cardiogenic factors (i.e., Wnt3a, BMP2), further acting on the colonies to direct the cells

toward a cardiogenic fate (Fig. 5). This molecular and cellular circuitry is likely to occur during the process of somatic cell reprogramming using Oct4 as the main reprogramming inducer, pointing to the importance of an accurate Oct4/Sox2 dosage in these experiments. Oct4 dosage within the nucleus is thus crucial to build specific bridges between different (i.e. Sox2 or Sox17) chromatin domains, resulting in generation of “transcription factories” working either to maintain ES cell pluripotency or to drive them toward a cardiogenic fate.

Materials and methods

Culture and cardiac commitment of Human Pluripotent stem cells.

Two HUES cell lines and one HUiPS cell line 11(Maherali et al., 2008) , using human dermal fibroblasts infected by lentivirus harbouring the cDNAs encoding Oct4, Sox2, Lin 28, Klf4 and Nanog, were used throughout this study without any difference in results. HUES-24 and HUES-9 pOct4/GFP (a transgenic cell line generated using BAC), and iPS cell were cultured on Mouse Embryonic Fibroblasts (MEF) prepared from E14 Mouse embryos as described (Tomescot et al. 2007). HUESC were treated for 48 hrs with 10 ng/ml BMP2 in the presence of 1 μM SU5402, a FGF receptor inhibitor, in KOSR-DMEM. HESC (both HUES-9 and HUES-24) were used within no more than 10 passages (P28-P38). Cells are phenotyped every 10 passages using anti-SSEA-3/4, TRA-1-60 and TRA-1-80 antibodies (Chemicon). Less than 5 % of cells were positive for SSEA-1 (Chemicon). Karyotype was found normal and stable in the course of the experiments.

EBs were generated from mock (GFP) -nucleofected or Oct4-iA-nucleofected in DMEM added with 20% FCS. Cells were let in suspension for 5d to allow for their aggregation and then EBs were plated on gelatin-coated dishes for the next 3 weeks.

The blocking anti-BMP2 and anti-Wnt3a antibodies (R &D systems MAB3552 and MAB1324, respectively), used at a concentration of 7.5 μg/ml medium, were added to mock or Oct4-iA-nucleofected cells for 2d prior to RNA extraction and RT-Q-PCR of Tbx6, Mesp1 and Tbx5 genes.

Real-Time Quantitative PCR by SYBR Green Detection.

RNA was extracted from ES cells using a Qiagen (Qiagen, Les Ullis, France) or Zymo Research (Orange, CA, USA, Proteingene, France) kit or a ZR RNA MicroPrep (Proteingene,

France) for singles colonies. 1 µg of RNA was reverse-transcribed using the SuperscriptII reverse transcriptase (Invitrogen, Cergy, France) and oligo(16)dT. Q-PCR was performed using a Light Cycler LC 1.5 or 480 (Roche Diagnostic) according to the manufacturer. Melting curves were used to determine the specificity of PCR products, confirmed using conventional gel electrophoresis and sequencing. Data were analysed according to Pfaffl (Pfaffl, 2001). Primers specific for human genes are described in Tomescot et al. (Tomescot et al., 2007) are available on request.

Primers to amplify enhancer/ promoter regions were:
Sox17 promoter: forward, 5'-actttcacagtccaggaacggagt-3' and reverse 5'-ggcttccttggagaaaggcaat-3' targeting a region within the 700 bp region upstream the transcription start site; Sox2: distal enhancer Forward, 5'-attagtctgctcttcctcggaatggttgg-3' and reverse ,5'-tgatgcttgttaaaaacgcttcgctcc-3'.
Nkx2.5 promoter: forward 5'-cagtcttgggagctcaagact-3' and reverse 5'-cagatccccaagcttactagc-3'
Tbx6 promoter: forward 5'-taacccgttcctgccccacct-3' and reverse 5'-tccgcttgagctccccccttcc-3'

Chromatin immunoprecipitation (ChIP) assay.

ChIP was performed according the Q2ChIP (Dahl and Collas, 2007) or Fast ChIP protocol (Nelson et al., 2006). Data were also confirmed using a standard ChIP procedure as previously described (Zeineddine et al., 2006). The antibodies used were anti-Oct4 (Santa Cruz sc-9081 and sc-5279), anti-Smad4 (Santa-Cruz sc-7966) and anti-H3triMeK4, triMeK27 and acetylK9 (UBI). Q-PCR was used to amplify the DNA elements as described above. Absolute enrichment was calculated assuming that at most 1% of nucleosome was immunoprecipitated (Dahl and Collas, 2007). Genomic region was thus considered enriched if 10 ng IP samples showed a greater enrichment when compared to 0.1 ng of input DNA. Data in all the text and figures are normalized to a control condition (absolute enrichment set to one) and are thus representative of a relative enrichment in one experimental condition (BMP2 treatment or Oct4 up-regulation) versus the control (non–treated cells or mock cells).

DNA constructs.

Human Sox17 ShRNA targeted the following Sox17 cDNA sequences gcaggtgaagcggctgaag. This was synthesised as a sense and antisense oligonucleotide, were annealed and subcloned in pSuper vector (Ambion). The DNA construct were nucleofected in HUESCs, using Amaxa specific nucleofector solution I, as recommended by the manufacturer.

Oct4-iA was amplified from RNA extracted from HESC as described in Lee et al (Lee et al., 2006) and subcloned in a pcDNA vector.

Cell Immunofluorescence and imaging

Cell immunofluorescence was carried out as previously described (Zeineddine et al., 2006). The anti-Sox17 antibody was from R&D (Mab1924). The Anti-Nkx2.5 antibody was from R&D (MAB2444 clone 259416), anti-Mef2c from Aviva, and Anti-CD31, CD45, CD34 were from Becton-Dickinson, the anti phospho-smad1/5/8 was from Cell Signaling Technology (#9511), the anti-β–catenin from BD Transduction Laboratories™ (#61015), the anti-sarcomeric actinin from SIGMA and the anti cTnt from Abcam (#ab45932). Slides were mounted using Fluoromount-G™ (ElectronMicroscopyScience).

Cardiac TnT and α-actinin florescent areas were measured in EBs using a thresholding and setting the cTnT and α-actinin fluorescent areas as regions of interest (ROI) within whole EBs observed at 4X magnification to measure the number of pixels within these ROIs with Image J software.

Images were acquired at room temperature using a Zeiss axioimager epifluorescence microscope using a Achroplan 10X objective (NA 0.25) (Fig1C), a Zeiss Axiostar microscope (N-Achroplan objective 20X, NA 0.45 (Fig. 1G) or a ZEISS laser-scanning LSM510Meta microscope (Achroplan objective 10X (NA 0.25) and Fluar 40x oil (NA 1.3) zoom 2x magnifications (Fig1H), and visualized without any processing by Zeiss LSM browser software or (Fig 2) a Biorad Multiphoton Radiance 2000MP microscope attached to a Nikon Eclipse with a 10x PL APO (NA 0.45) at room temperature and visualized with Biorad software and Image J without any processing.

FACS analysis. HESC were trypsinised and washed twice with PBS, filtered through a 70 μm mesh filter before FACS analysis using FACS Calibur (Becton Dickinson) and CELL QUEST software.

Protein immunoprecipitation and Western blots. END-2 cells were cultured in DMEM, supplemented with 10% FCS. Cells were nucleofected with Oct4-iA cDNA using the kit V (Amaxa). Cells were lysed in RIPA buffer. Co-Immunoprecipitation was performed in RIPA buffer and Western blot analysis was conducted as previously reported (Puceat et al., 1998). The anti-Oct4 antibodies used were from Santacruz (N19 and H134).
Sox2 and Oct4 western blots were performed using the anti-Sox2 from Santacruz (Y17) and anti-Oct4 (H-134) recognising both Oct4-iA and iB.

Screening of immunostained cells by High Content imaging.
Immunofluorescence scan of BMP2-treated HUES-9 pOct4/GFP or Oct4iA nucleofected HESC stained with anti-Sox17 and alexa546 conjugated anti-Mouse IgG- or anti–Mesp2 and anti-alexa-680 conjugated anti-rabbit IgG antibodies or anti-Nkx2.5 and anti-alexa-488 conjugated anti-rabbit IgG antibodies or anti-Mef2c and anti-alexa-488 conjugated anti-mouse IgG antibodies: HESC were plated in 96 wells plates on MEF and treated or not with 10 ng/ml BMP2 and SU5402 for 4 d. Other cells were nucleofected with Oct4iA cDNA and plated in labtech. After immunostaining, the HC imaging 96 wells plates (cells in PBS) were scanned using the Arrayscan (Cellomics ThemoFisher attached to a Zeiss inverted microscope and using 20X N-Achroplan objective, NA 0.45, at room temperature) using the Cell Health Profiling Bioapplication. The fluorescence threshold was determined from the background obtained in non BMP2-stimulated cells or mock cells and set as a fixed threshold value to scan the wells of BMP2-treated cells or Oct4iA-nucleofected cells. In BMP2 experiments, 50 fields/well and 32 wells were scanned giving a total of 98120 cells selected according the morphology, size and the proximity of their nuclei (i.e. to discriminate HESC colonies from feeder cells). Different types of events were scored using the cell feature parameters and the Boolean operators. The visualisation of images and analysis were then performed using the vHCS software.

Online Supplemental material

S1: Characterization of HUES-9 pOct4/GFP clone. Non-cardiac potential of differentiation of Oct4-OEC. KO of Sox2/Sox17 and consequences on BMP2-induced gene expression

S2: Paracrine action of Oct4-overexpressing cells

S3: Oct4 overexpressing cells activate smad and β-catenin pathways; The Oct4/Sox17 network is conserved in iPSCs.

We thank Dr Ng HH (Genome Institute of Singapore) for the gift of Sox2 ShRNA plasmid, Drs M Mitjavila and N Lefort for help in FACS analysis, Y Maury (INSERM-UMR861) for help in HC imaging, O Guillevic, L Hamon and G Blin for experimental help, Drs A Terzic (Mayo Foundation, Rochester, USA), HH Ng (Biopolis Singapore) and R Feil (CNRS Montpellier, France) for critical reading of the MS, Dr M. Buckingham (Pasteur Institute, Paris) for her invaluable comments on the MS the National Agency for Research (ANR, programmes Blanc, HUES signature and Specistem) and Genopole for funding this research. SS and DN were funded by ANR.

References

Bakre, M.M., A. Hoi, J.C. Mong, Y.Y. Koh, K.Y. Wong, and L.W. Stanton. 2007. Generation of multipotential mesendodermal progenitors from mouse embryonic stem cells via sustained Wnt pathway activation. *J Biol Chem.* 282:31703-12.

Ben-Shushan, E., H. Sharir, E. Pikarsky, and Y. Bergman. 1995. A dynamic balance between ARP-1/COUP-TFII, EAR-3/COUP-TFI, and retinoic acid receptor:retinoid X receptor heterodimers regulates Oct-3/4 expression in embryonal carcinoma cells. Mol Cell Biol. 15:1034-48.

Bondue, A., G. Lapouge, C. Paulissen, C. Semeraro, M. Iacovino, M. Kyba, and C. Blanpain. 2008. Mesp1 acts as a master regulator of multipotent cardiovascular progenitor specification. *Cell Stem Cell.* 3:69-84.

Chew, J.L., Y.H. Loh, W. Zhang, X. Chen, W.L. Tam, L.S. Yeap, P. Li, Y.S. Ang, B. Lim, P. Robson, H.H. Ng,. 2005. Reciprocal transcriptional regulation of Pou5f1 and Sox2 via the Oct4/Sox2 complex in embryonic stem cells. *Mol Cell Biol*. 25:6031-46.

Crease, D.J., S. Dyson, and J.B. Gurdon. 1998. Cooperation between the activin and Wnt pathways in the spatial control of organizer gene expression. *Proc Natl Acad Sci U S A.* 95:4398-403.

Dahl, J.A., and P. Collas. 2007. Q2ChIP, a quick and quantitative chromatin immunoprecipitation assay, unravels epigenetic dynamics of developmentally regulated genes in human carcinoma cells. *Stem Cells.* 25:1037-46.

Hoffman, L.M., and M.K. Carpenter. 2005. Characterization and culture of human embryonic stem cells. *Nat Biotechnol.* 23:699-708.

Kasai, M., K. Satoh, and T. Akiyama. 2005. Wnt signaling regulates the sequential onset of neurogenesis and gliogenesis via induction of BMPs. *Genes Cells.* 10:777-83.

Lee, J., H.K. Kim, J.Y. Rho, Y.M. Han, and J. Kim. 2006. The human OCT-4 isoforms differ in their ability to confer self-renewal. *J Biol Chem.* 281:33554-65..

Liu, Y., M. Asakura, H. Inoue, T. Nakamura, M. Sano, Z. Niu, M. Chen, R.J. Schwartz, and M.D. Schneider. 2007. Sox17 is essential for the specification of cardiac mesoderm in embryonic stem cells. *Proc Natl Acad Sci U S A.* 104:3859-64.

Loh, Y.H., Q. Wu, J.L. Chew, V.B. Vega, W. Zhang, X. Chen, G. Bourque, J. George, B. Leong, J. Liu, K.Y. Wong, K.W. Sung, C.W. Lee, X.D. Zhao, K.P. Chiu, L. Lipovich, V.A. Kuznetsov, P. Robson, L.W. Stanton, C.L. Wei, Y. Ruan, B. Lim, and H.H. Ng. 2006. The Oct4 and Nanog transcription network regulates pluripotency in mouse embryonic stem cells. *Nat Genet.* 38:431-40.

Maherali, N., T. Ahfeldt, A. Rigamonti, J. Utikal, C. Cowan, and K. Hochedlinger. 2008. A high-efficiency system for the generation and study of human induced pluripotent stem cells. *Cell Stem Cell.* 3:340-5.

Menard, C., C. Grey, A. Mery, D. Zeineddine, F. Aimond, and M. Puceat. 2004. Cardiac specification of embryonic stem cells. *J Cell Biochem.* 93:681-687.

Mummery, C.L., T.A. van Achterberg, A.J. van den Eijnden-van Raaij, L. van Haaster, A. Willemse, S.W. de Laat, and A.H. Piersma. 1991. Visceral-endoderm-like cell lines induce differentiation of murine P19 embryonal carcinoma cells. *Differentiation.* 46:51-60.

Naito, A.T., I. Shiojima, H. Akazawa, K. Hidaka, T. Morisaki, A. Kikuchi, and I. Komuro. 2006. Developmental stage-specific biphasic roles of Wnt/beta-catenin signaling in cardiomyogenesis and hematopoiesis. *Proc Natl Acad Sci U S A.* 103:19812-7.

Nelson, J.D., O. Denisenko, and K. Bomsztyk. 2006. Protocol for the fast chromatin immunoprecipitation (ChIP) method. *Nat Protoc.* 1:179-85.

Niwa, H. 2007. How is pluripotency determined and maintained? *Development.* 134:635-46.

Niwa, H., J. Miyazaki, and A.G. Smith. 2000. Quantitative expression of Oct-3/4 defines differentiation, dedifferentiation or self-renewal of ES cells. *Nat Genet*. 24:372-6.

Nostro, M.C., X. Cheng, G.M. Keller, and P. Gadue. 2008. Wnt, activin, and BMP signaling regulate distinct stages in the developmental pathway from embryonic stem cells to blood. *Cell Stem Cell.* 2:60-71.

Peerani, R., B.M. Rao, C. Bauwens, T. Yin, G.A. Wood, A. Nagy, E. Kumacheva, and P.W. Zandstra. 2007. Niche-mediated control of human embryonic stem cell self-renewal and differentiation. *Embo J.* 26:4744-55. Epub 2007 Oct 18.

Pfaffl, M.W. 2001. A new mathematical model for relative quantification in real-time RT-PCR. *Nucleic Acids Res*. 29:e45.

Puceat, M., S. Roche, and G. Vassort. 1998. Src family tyrosine kinase regulates intracellular pH in cardiomyocytes. *J Cell Biol*. 141:1637-46.

Seguin, C.A., J.S. Draper, A. Nagy, and J. Rossant. 2008. Establishment of endoderm progenitors by SOX transcription factor expression in human embryonic stem cells. *Cell Stem Cell.* 3:182-95.

Smith, A.G. 1991. Culture and diffrentiation of embryonic stem cells. *J. Tiss. Cult. meth.* 13:89-94.

Sumi, T., N. Tsuneyoshi, N. Nakatsuji, and H. Suemori. 2008. Defining early lineage specification of human embryonic stem cells by the orchestrated balance of canonical Wnt/{beta}-catenin, Activin/Nodal and BMP signaling. *Development.* 135:2969-79.

Takahashi, K., K. Tanabe, M. Ohnuki, M. Narita, T. Ichisaka, K. Tomoda, and S. Yamanaka. 2007. Induction of pluripotent stem cells from adult human fibroblasts by defined factors. *Cell.* 131:861-72.

Tam PPL, and G. Schoenwolf. 1999. Cardiac fate map: lineage, allocation, morphogenetic movement and cell commitment. *Heart Development*:3-18.

Tomescot, A., J. Leschik, V. Bellamy, G. Dubois, E. Messas, P. Bruneval, M. Desnos, A. Hagège, J. Itskovitz-Eldor, P. Menasché, and M. Pucéat. 2007. Differentiation in vivo of cardiac committed Human embryonic stem cells in post-myocardial infarcted rats. *Stem Cells.* 25:2200-5.

Yamanaka, S. 2007. Strategies and new developments in the generation of patient-specific pluripotent stem cells. *Cell Stem Cell.* 1:39-49.

Zeineddine, D., E. Papadimou, K. Chebli, M. Gineste, J. Liu, C. Grey, S. Thurig, A. Behfar, V.A. Wallace, I.S. Skerjanc, and M. Puceat. 2006. Oct-3/4 dose dependently regulates specification of embryonic stem cells toward a cardiac lineage and early heart development. *Dev Cell.* 11:535-46.

Zorn, A.M., G.D. Barish, B.O. Williams, P. Lavender, M.W. Klymkowsky, and H.E. Varmus. 1999. Regulation of Wnt signaling by Sox proteins: XSox17 alpha/beta and XSox3 physically interact with beta-catenin. *Mol Cell.* 4:487-98.

Abbreviations used in this paper: d, days; ICM, inner cell mass ; RT-Q-PCR, real-time Quantitative PCR; TF, transcription factor; *p*, promoter; Oct4-iA-OEC, Oct4-iA overexpressing cells ; CM, conditioned medium; WB, Western Blot; cTnT, cardiac troponin T; Histone H3, H3. IF, immunofluorescence; EB, embryoïd bodies; WCL, whole cell lysate, NA, numerical aperture. HCC imaging, High Content Cell imaging.

Figure 1. **Over-expression of Oct4-iA induces cardiogenesis.**

HESC 24 **(**A**)** or HUES-9 pOct4/GFP (B) ctrl or treated for 48 hrs with BMP2. (A) *Oct4* isoforms Q-PCR. (B) Q-PCR *of GFP* cDNA. (n=2-3). (C) GFP FACS in HUES-9 pOct4/GFP cells (upper) non-treated (left) or treated (right) with BMP2. (D,E,F) Cells nucleofected with *Oct4-iA* or *pCMV-GFP* and cultured for 4d. (D) FACS of GFP (nucleofection efficiency: inset) and SSEA-1 in mock cells (pcDNA backbone, left panel) and Oct4-iA-OEC (right panel) (E) Q-PCR of induced genes (F) Q-PCR of *Sox17* and *Hex* (amplicons on gel). (means ± SEM (n =3-6) normalised to huGAPDH). * statistically significant ($p \leq 0.01$). (G) IF anti-Sox17, -Mef2c and -Nkx2.5 of Oct4-iA OEC scanned by an arrayscan. Bars: 20 μm. (H) IF anti-sarcomeric actinin and anti-cTnT of day 30 EBs generated from mock or Oct4-iA OEC.

Figure 2. **Oct4 interaction with Sox17 promoter and protein at the expense of Sox2**

Ctrl HUESC or treated for 48 hrs with BMP2, and used for anti-Oct4 ChIP. *Sox2* distal enhancer (pSox2) (A) or *Sox17p* (p*Sox17*) (B) were amplified in RT-Q-PCR (products on gel, insets). Right Inset in B: RT-Q-PCR for *Sox17* in cells treated or not with BMP2. (C and D) anti-Oct4 ChIP in *Oct4-iA*-OECs. p*Sox2* or p*Sox17* was amplified in Q-PCR. (n=3 means±SEM). (E) Anti-H3trimeK4, -H3trimeK27 and -H3acetylK9 ChIP in *Oct4-iA*-OECs. pSoxs were amplified in Q-PCR. Results are expressed as enrichment (H3AcK9) or as a ratio of enrichment (K4/K27). Data are normalised to inputs and to controls (chromatin from GFP-nucleofected cells) from 2 experiments (median ± errors). (F) Anti-Sox2 WB from ctrl or Oct4-iA-OEC chromatin. (G) IF anti-Sox17 and dapi in Ctrl or BMP2-stimulated HESC. (H) anti-Oct4 ChIP analysis of p*Sox17*. Cells were nucleofected with GFP cDNA (Ctrl) or Oct4-iA cDNA alone or together with *Sox2* cDNA or *Sox2* ShRNA prior to ChIP. Q-PCR of p*Sox17* (gel of amplicons on the left). The enrichment in ShRNASox2^{+} Oct4-OEC was normalized to the one of Oct4-iA-OEC (set to 1). Results are expressed as the median ±errors

from 2 experiments. (I) END-2 cells expressing Sox17 were nucleofected with Oct4-iA and cultured for 2 d. IP anti-Oct4 and WB anti-Sox17. END-2 WCL was run as a positive control.

Figure 3. **Sox17 mediates Oct4-triggered cardiogenic commitment of HUESC.** *Oct4-iA* cDNA alone or together with Sox17 ShRNA was nucleofected in HESC (A) Q-PCR of genes (n=3). **(**B**)** Anti-Oct4ChIP-Q-PCR analysis of *Sox2* distal enhancer and *Sox17p*. (n=3, mean± SEM).

Figure 4. **Over-expression of Oct4-iA induces secretion of paracrine factors**

(A) Q-PCR of genes (n=3-5) (B) anti-Oct4 ChIP analysis of *Sox2* distal enhancer and *Sox17p* (pSox) in wt HESC treated for 4d with CM of Oct4-iA-OEC. CM from GFP-nucleofected mock cells was used as control (experiment in duplicate). (C) HESC nucleofected with *Oct4-iA* or *GFP* (mock cells) and cultured for 4d in the absence (ctrl) or presence of DKK, Noggin or Lefty. (D) Q-PCR of *BMP2* and *Wnt3a* in Oct4iA-OEC (E) anti-Sox17 and -Mesp2 IF of ctrl and BMP2-treated HUES-9 pOct4/GFP cells. (F) Venn diagram for the number of cells positive for GFP, Sox17 and Mesp2 only or together. Ctrl or BMP2 challenged HUES-9 pOct4/GFP cells in 96 wells plates were stained with anti-Sox17 and –Mesp2 antibodies. Numbers in the diagram indicate the total number of cells and the percentage. * significantly different from control ($p \leq 0.001$).

Figure 5. **The Sox17/Oct4 circuit is functional within a stem cell colony or "niche"**.
Oct4 and Sox17 work in combination to drive HuPSC toward an mesendodermal fate, and through secretion of BMP2 and wnt3a toward the fate of cardiac progenitors.

JCB MS# 200901040R2

Supplementary figure 1: characterization of HUES9 pOct4GFP clone. Non-cardiac potential of differentiation of Oct4-OEC. KO of Sox2/Sox17 and consequences on BMP2-induced gene expression

(A) HUES-9 pOct4/GFP cell line: Left image: mock cell clone; middle and right images: HUES cells expressing COUP-TFI. Raw images were acquired using a ZEISS laser scanning LSM510Meta microscope at 20X (NA 0.75) and visualized using the LSM software.

(B) HUES-9 pOct4/GFP cell line was nucleofected or not (Ctrl) with Oct4-iA and RNA was extracted 2 days later to carry-out a RT-real time PCR of GFP.

(C) FACS analysis of mock (Ctrl) or Oct4-iA over-expressing HUES cells (Oct4-iA) Cells were stained with and anti-CD31, CD34, or CD45 antibodies.

(D) Real time PCR of *Sox2* cDNA reversed transcribed from RNA extracted from control (mock GFP-nucleofected cells), Sox2 ShRNA nucleofected cells (ShSox2) and Sox2 nucleofected cells (n=2).

(E) anti-Sox2 Western blot of 50 μg proteins extracted from control or shRNA Sox2 nucleofected HUES cells using an anti-Sox2 antibody (santa-cruz Sc17310).

(F) Expression of Oct4-iA and Sox 17 was monitored by western blot. Anti-Oct4-iA and –Sox17 Western blot of 50 μg proteins extracted from control or Oct4-iA nucleofected HUES cells with or without Sox17 ShRNA, using an anti C terminal Oct-3/4 (sc 5279) or anti-Sox17 (R&D) antibody. Blots are normalised with an anti-tubulin antibody.

(G) Mock nucleofected cells or cells nucleofected with *Sox17* ShRNA were stimulated with BMP2 and SU5402 for 4 days, RNA extracted and mesodermal and cardiac gene monitored by RT-Q-PCR (n=2). Right panel: *Sox17* expression was monitored by Q-PCR and the amplicon run on gel.

Supplementary figure 2 : **Paracrine action of Oct4 overexpressing cells**

HUES-9 pOct4/GFP cells nucleofected with Oct4-iA cDNA and wt mock cells were mixed together in the same wells at different ratios (1:1; 3:1; 9:1). After 4 days of coculture, wt mock cell colonies were dissected out and used in real time PCR (A) or (B) cells were fixed and stained with an anti-Nkx2.5 antibody.

(A) PCR data are normalised to expression of the housekeeping gene GAPDH and expressed as fold increased compared to wild type HUES cells (ratio 0:1).

(B) The left panels show dapi, the middle, GFP, and the right, Nkx2.5. The insets, magnifications of a ROI within non-GFP cells shows the nuclear staining or just non specific cytosolic background in control wt cells. The top panels illustrate a well with cells mixed at 3:1 ratio, the middle one, a well with cells mixed at 9:1 ratio and the bottom only wt cells. The experiment was performed in duplicate with similar results. Images were acquired at room temperature using a laser-scanning LSM510Meta Zeiss microscope at 40X oil Fluar objective (NA 1.3) ; images were visualized using the Zeiss LSM software. Scale 20 µm.

(C) Real time PCR of RNA extracted from control, BMP2- treated or Wnt3a and BMP2-treated HUES cells.

Early cardiac marker genes as well as BMP2 and Wnt3a mRNA (inset) were amplified in real time PCR. Data are normalised to human GAPDH expression and expressed as means ± SEM (n = 3-5). * significantly different from control ($p \leq 0.001$).

Supplementary figure 3 : **Oct4 overexpressing cells activate smad and β-catenin pathways. The Oct4/Sox17 network is conserved in iPSCs**

(A) HUES cells (control (Ctrl) or overexpressing Oct4-iA (Oct-4iA)) were subjected to ChIP assay using an anti-smad 4 antibody. Real-time PCR was used to amplify the Nkx2.5 and Tbx6 promoter regions. Results are expressed as log(2) enrichment assuming that 1% nucleosome were immunoprecipitated.

(B) HUES cells (control (Ctrl) or overexpressing Oct-4iA (Oct-4iA)) were fixed and stained 2 days after nucleofection using an anti-phospho smad1/5/8 or anti-β-catenin antibody and with dapi. Raw images were acquired at room temperature using a Zeiss axioimager epifluorescence microscope at 10X achroplan (NA 0.25) and a Axiocam CCD and visualized using axiovision software. Scale bar 20 μm.

(C) Colonies of wild type (Ctrl, left panel) and Oct4-iA over-expressing (+Oct4-iA right panel) iPSC cultured in the presence of FGF2 visualised at room temperature using a zeiss axiovert microscope at 10x Achroplan (NA 0.25) and an Axiocam CCD ; Images were visualized without any processing with the Axiovision software . Scale bar 20 μm (D) iPSCs were transfected with Oct4-iA or GFP as a control and gene expression was monitored 6 days later by RT-Q-PCR. Data are normalised to GAPDH expression and expressed as means ± SEM (n = 3-5). * significantly different from control ($p \leq 0.001$). The inset shows the gel of the Sox17 and GAPDH amplicons following real time PCR. (E) ChIP analysis of Sox2 and Sox17 DNA promoter region (pSox) co-immunoprecipitated with an anti-Oct4 antibody in iPSCs over-expressing Oct4-iA. Data are normalised to GAPDH DNA (input) and fold changes compared to mock cells (GFP-nucleofected) and expressed as means ± SEM (n = 3-5). (F) RT-Q-PCR of BMP2 and Wnt3a mRNA in control and Oct4-iA expressing HUES cells. Data are normalised to

GAPDH expression and expressed as means ± SEM (n = 3-5). * significantly different from control ($p \leq 0.001$).

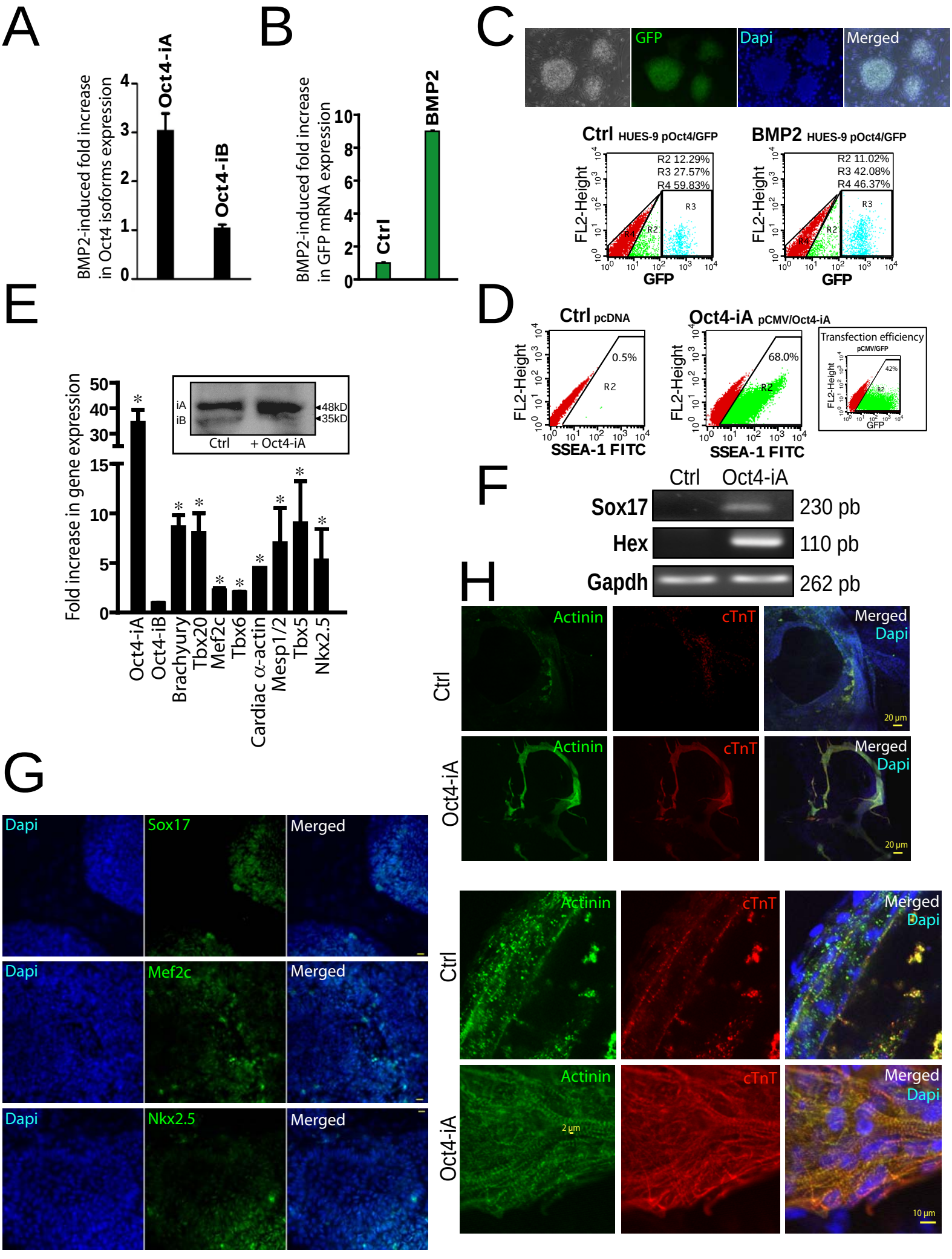

A
BMP2-induced fold increase in Oct4 isoforms expression
Oct4-iA
Oct4-iB
B
BMP2-induced fold increase in GFP mRNA expression
Ctrl
BMP2
C
GFP
Dapi
Merged
Ctrl HUES-9 pOct4/GFP
BMP2 HUES-9 pOct4/GFP
R2 12.29%
R3 27.57%
R4 59.83%
R2 11.02%
R3 42.08%
R4 46.37%
FL2-Height
GFP
D
Ctrl pcDNA
Oct4-iA pCMV/Oct4-iA
0.5%
68.0%
SSEA-1 FITC
Transfection efficiency
pCMV/GFP
42%
E
Fold increase in gene expression
iA
iB
48kD
35kD
Ctrl
+ Oct4-iA
Oct4-iA
Oct4-iB
Brachyury
Tbx20
Mef2c
Tbx6
Cardiac α-actin
Mesp1/2
Tbx5
Nkx2.5
F
Ctrl
Oct4-iA
Sox17
230 pb
Hex
110 pb
Gapdh
262 pb
G
Dapi
Sox17
Merged
Mef2c
Nkx2.5
H
Actinin
cTnT
Merged
Dapi
Ctrl
Oct4-iA
20 µm
2 µm
10 µm

Figure 1

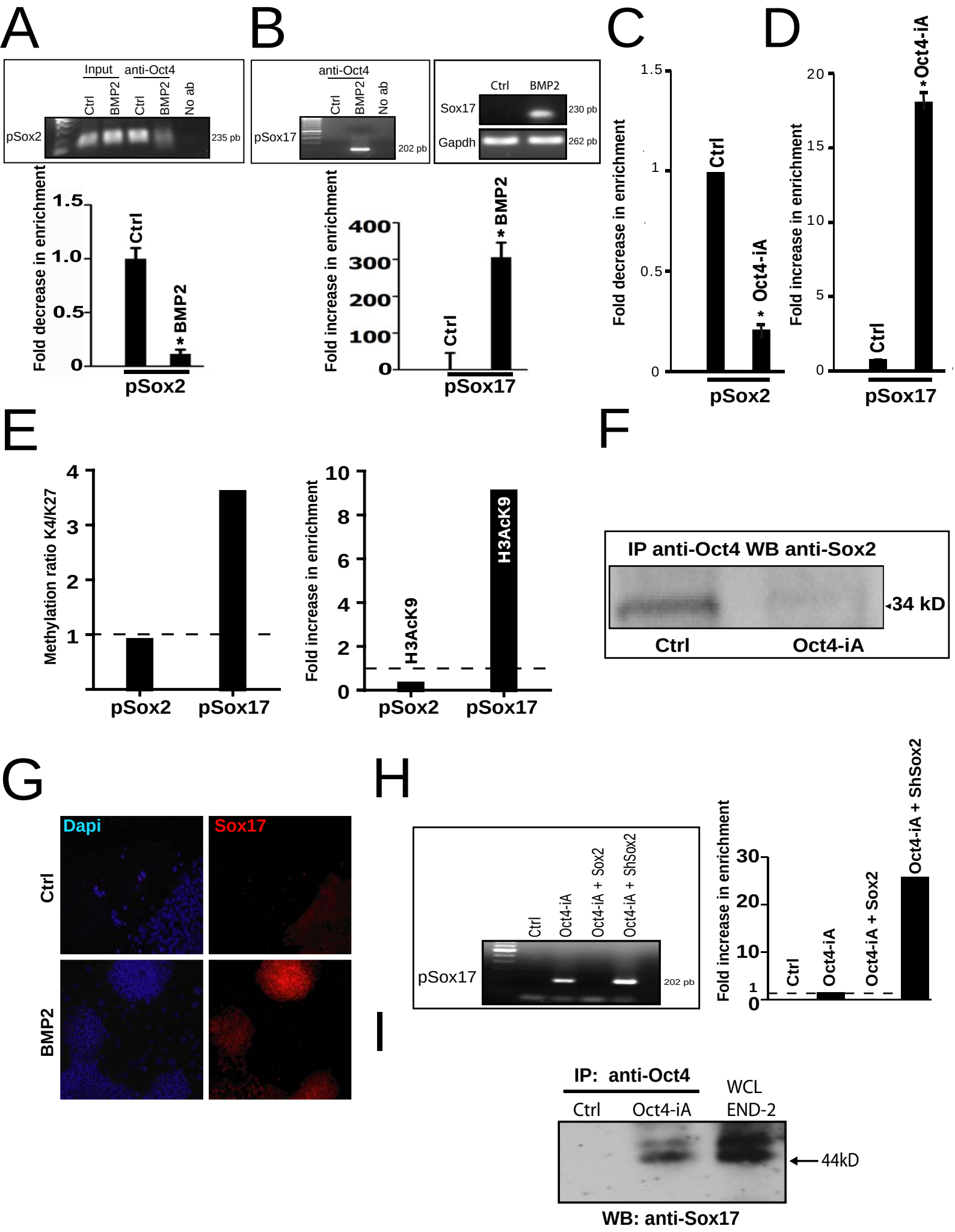
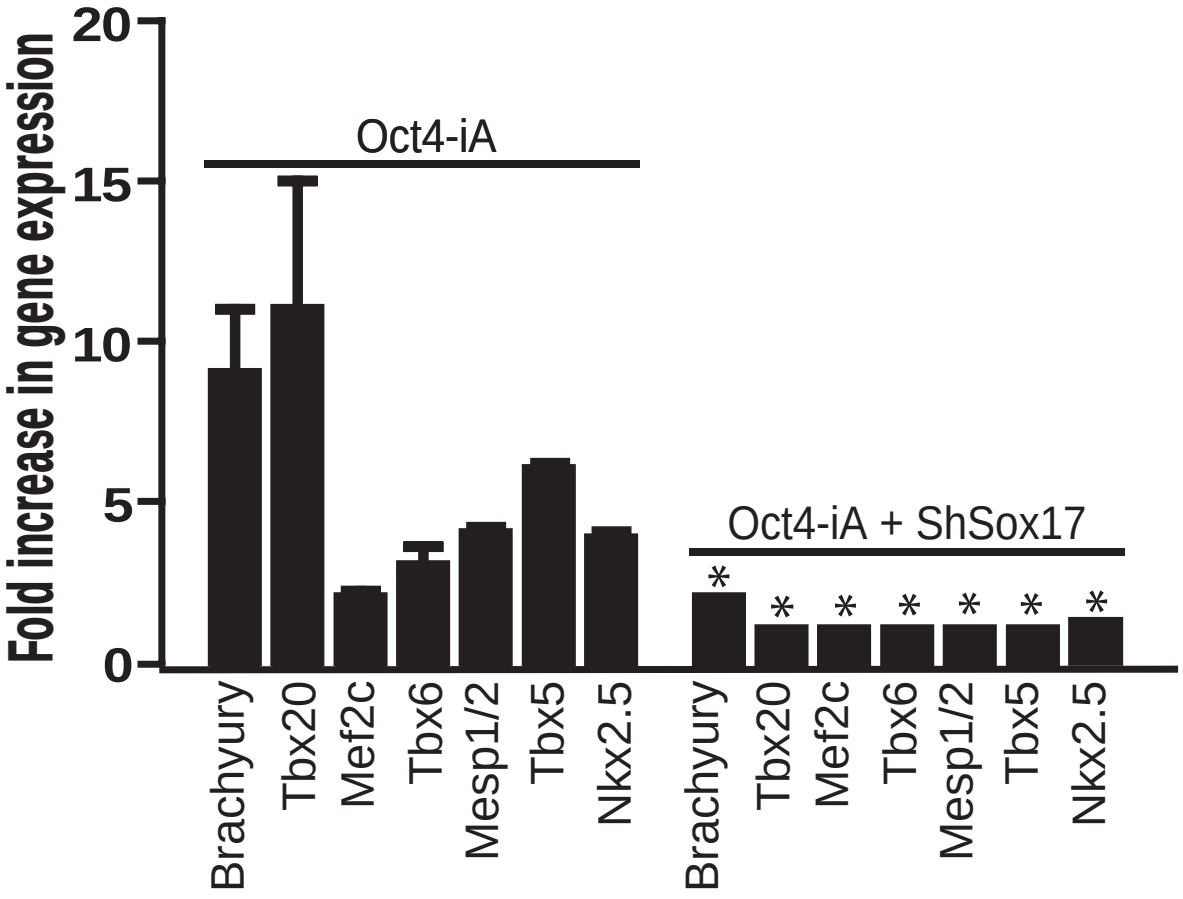

A
Input
anti-Oct4
Ctrl
BMP2
Ctrl
BMP2
No ab
pSox2
235 pb
Fold decrease in enrichment
1.5
1.0
0.5
0
Ctrl
* BMP2
pSox2
B
anti-Oct4
Ctrl
BMP2
No ab
pSox17
202 pb
Ctrl
BMP2
Sox17
230 pb
Gapdh
262 pb
Fold increase in enrichment
400
300
200
100
0
Ctrl
* BMP2
pSox17
C
Fold decrease in enrichment
1.5
1
0.5
0
Ctrl
* Oct4-iA
pSox2
D
Fold increase in enrichment
20
15
10
5
0
Ctrl
* Oct4-iA
pSox17
E
Methylation ratio K4/K27
4
3
2
1
pSox2
pSox17
Fold increase in enrichment
10
8
6
4
2
0
H3AcK9
H3AcK9
pSox2
pSox17
F
IP anti-Oct4 WB anti-Sox2
34 kD
Ctrl
Oct4-iA
G
Dapi
Sox17
Ctrl
BMP2
H
Ctrl
Oct4-iA
Oct4-iA + Sox2
Oct4-iA + ShSox2
pSox17
202 pb
Fold increase in enrichment
30
20
10
1
0
Ctrl
Oct4-iA
Oct4-iA + Sox2
Oct4-iA + ShSox2
I
IP: anti-Oct4
Ctrl
Oct4-iA
WCL
END-2
44kD
WB: anti-Sox17

Figure 2

A


Fold increase in gene expression
20
15
10
5
0
Oct4-iA
Oct4-iA + ShSox17
*
Brachyury
Tbx20
Mef2c
Tbx6
Mesp1/2
Tbx5
Nkx2.5

B

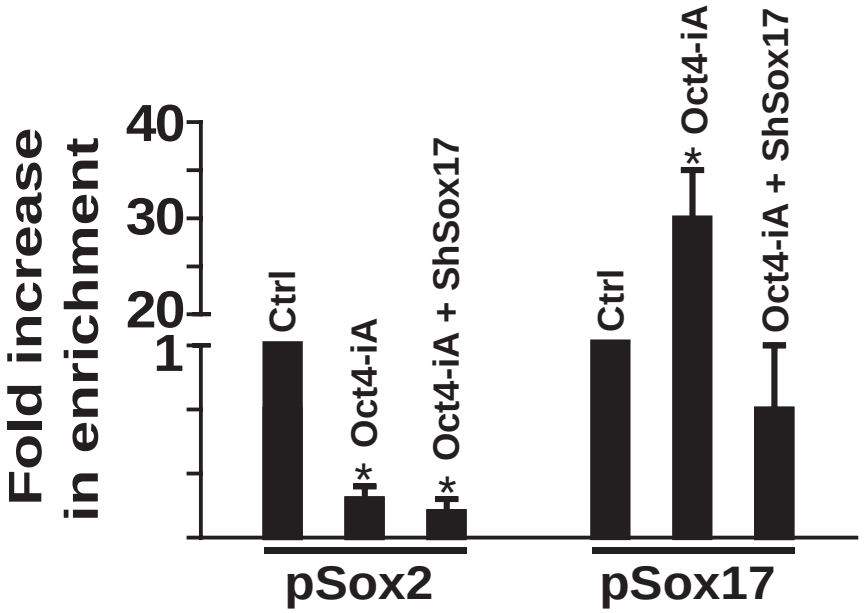

Fold increase in enrichment
40
30
20
1
Ctrl
* Oct4-iA
* Oct4-iA + ShSox17
pSox2
pSox17

Figure 3

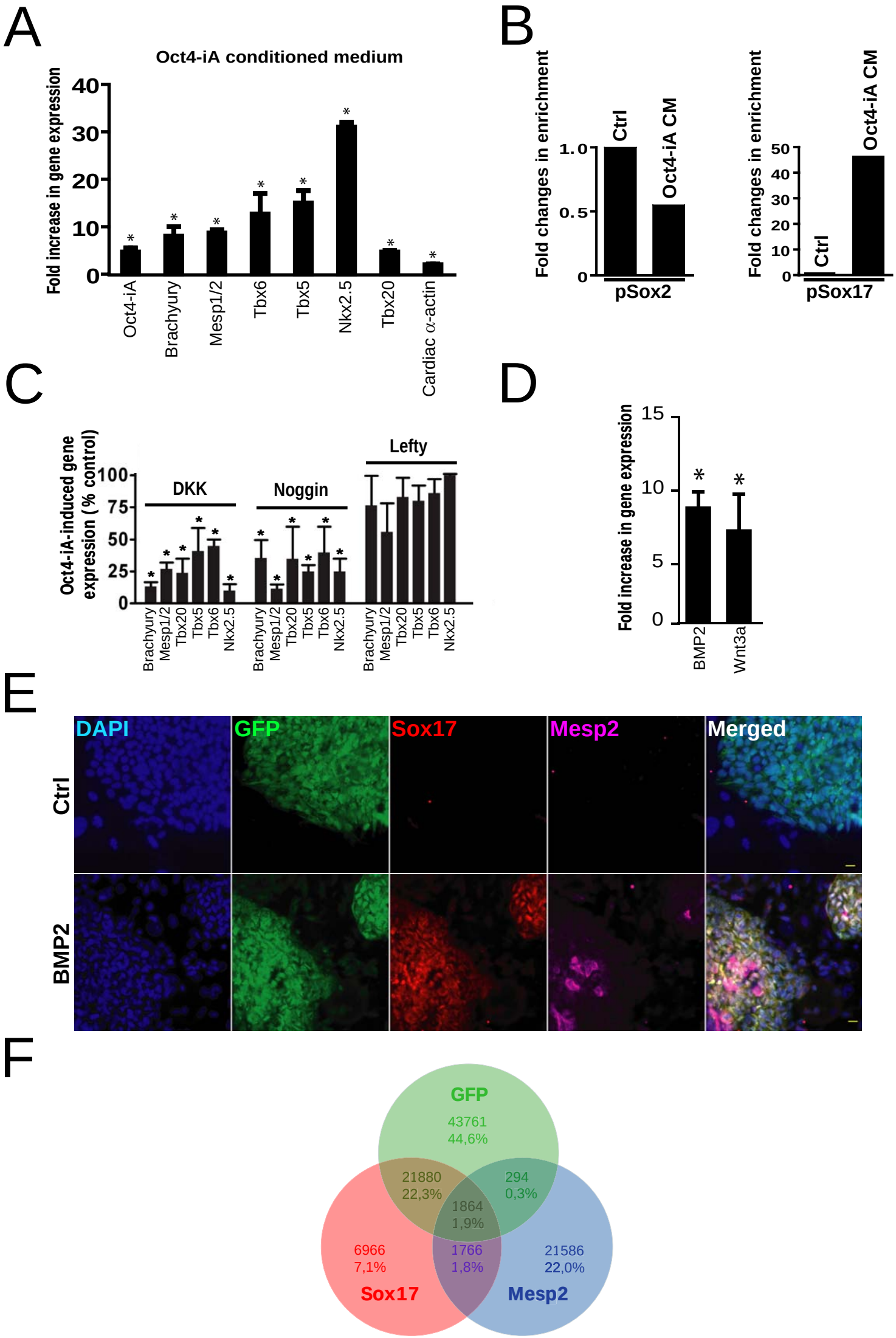

A
Oct4-iA conditioned medium
Fold increase in gene expression
40
30
20
10
0
Oct4-iA
Brachyury
Mesp1/2
Tbx6
Tbx5
Nkx2.5
Tbx20
Cardiac α-actin
B
Fold changes in enrichment
1.0
0.5
0
Ctrl
Oct4-iA CM
pSox2
Fold changes in enrichment
50
40
30
20
10
0
Ctrl
Oct4-iA CM
pSox17
C
Oct4-iA-induced gene expression (% control)
100
75
50
25
0
DKK
Noggin
Lefty
Brachyury
Mesp1/2
Tbx20
Tbx5
Tbx6
Nkx2.5
D
Fold increase in gene expression
15
10
5
0
BMP2
Wnt3a
E
DAPI
GFP
Sox17
Mesp2
Merged
Ctrl
BMP2
F
GFP
43761
44,6%
21880
22,3%
294
0,3%
1864
1,9%
6966
7,1%
1766
1,8%
21586
22,0%
Sox17
Mesp2

Figure 4

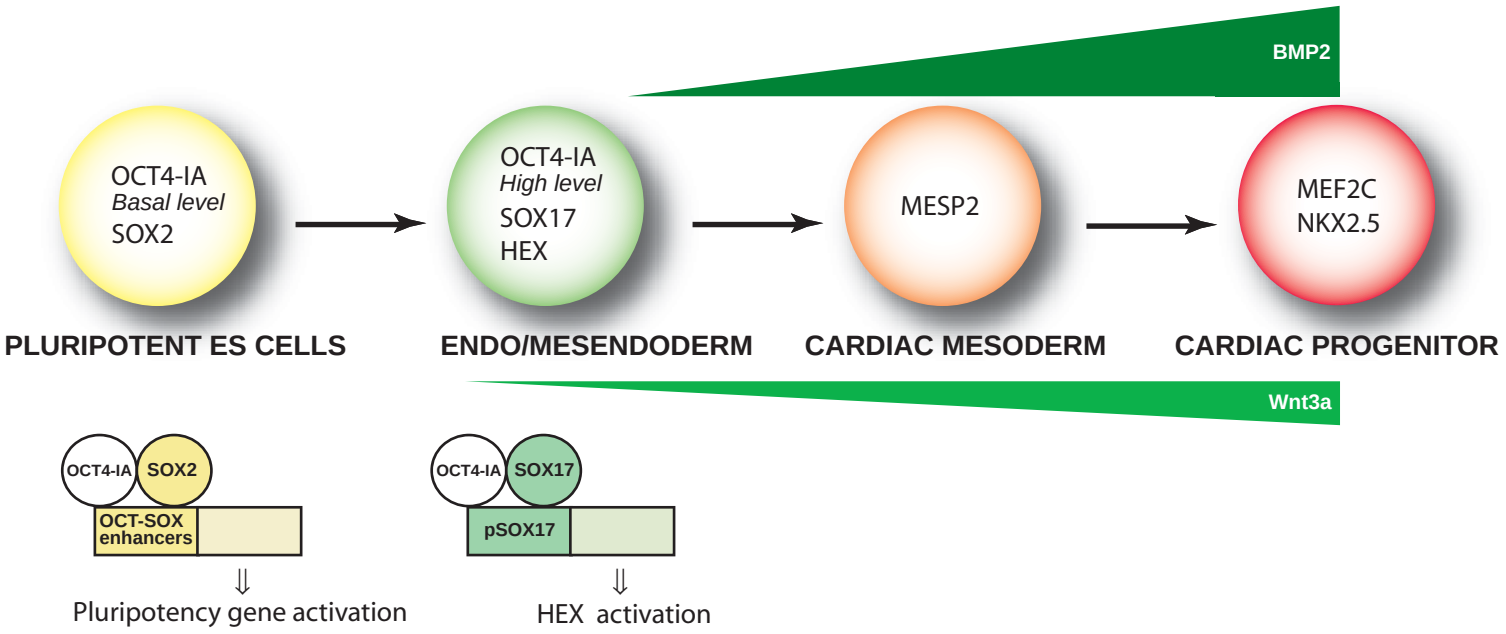
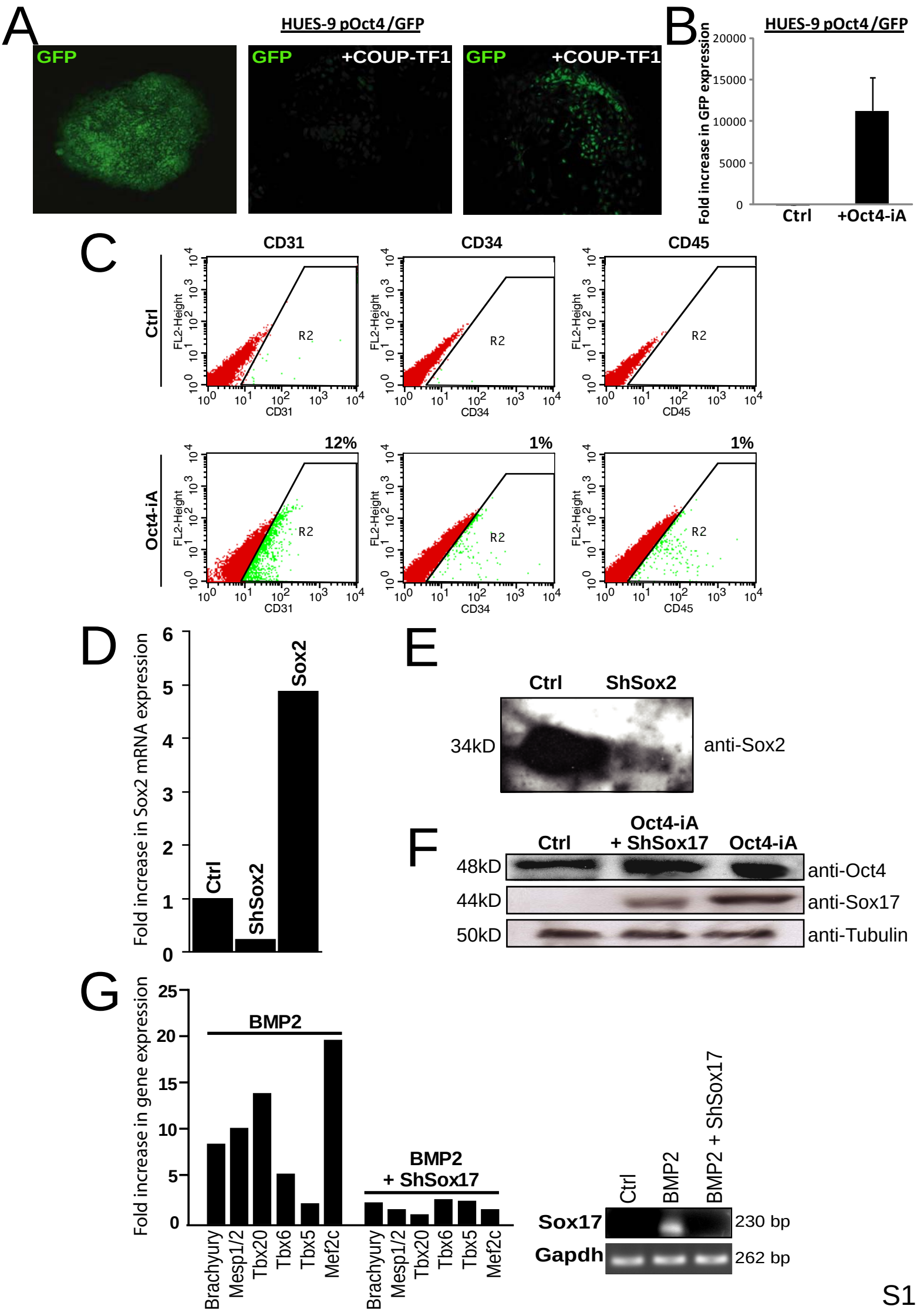
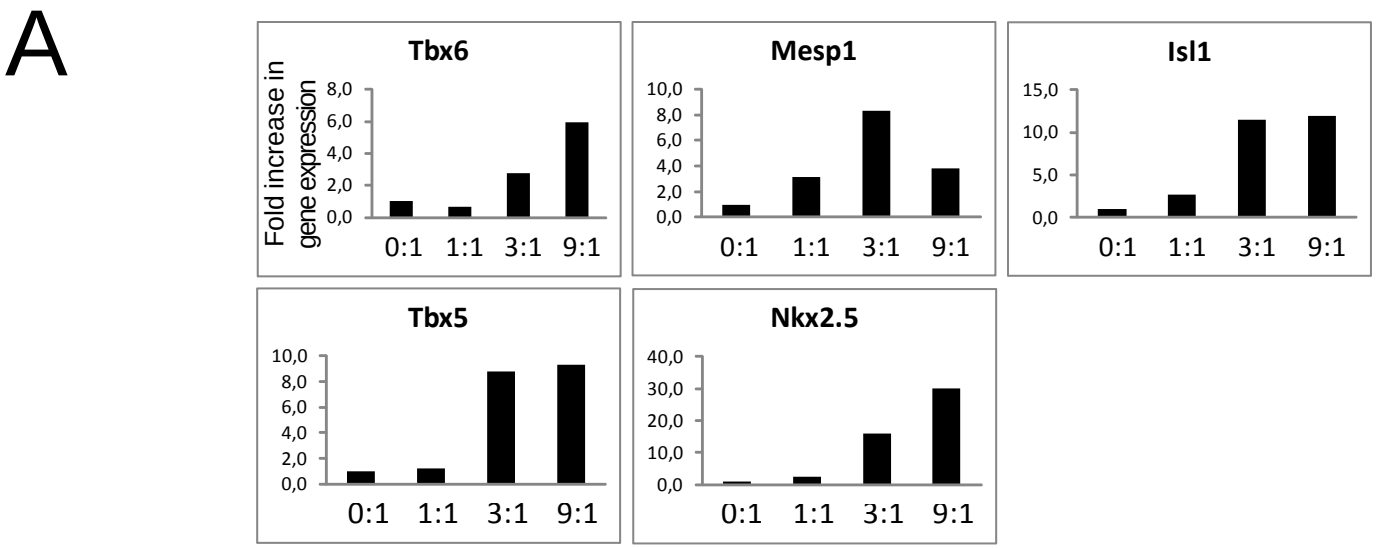
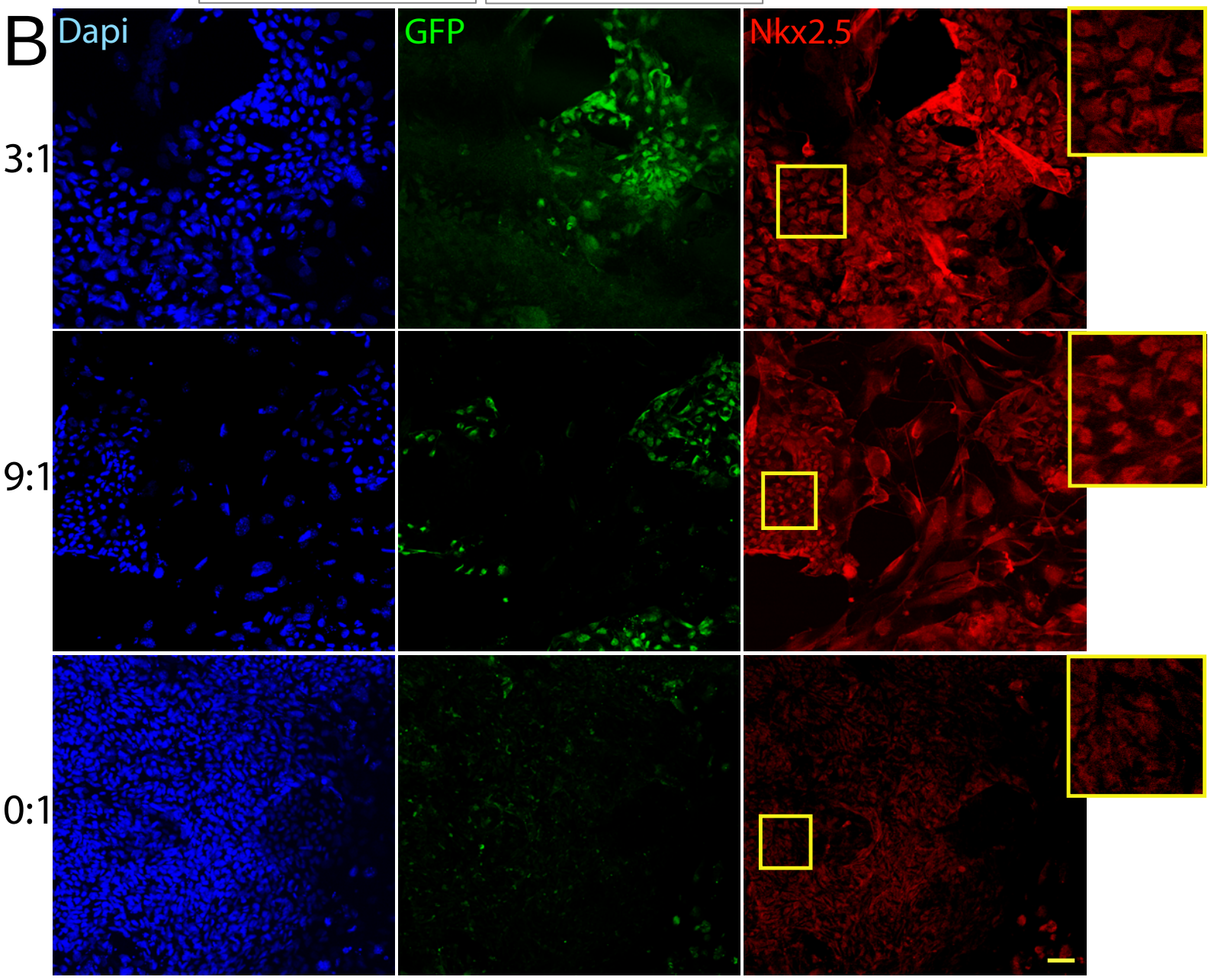
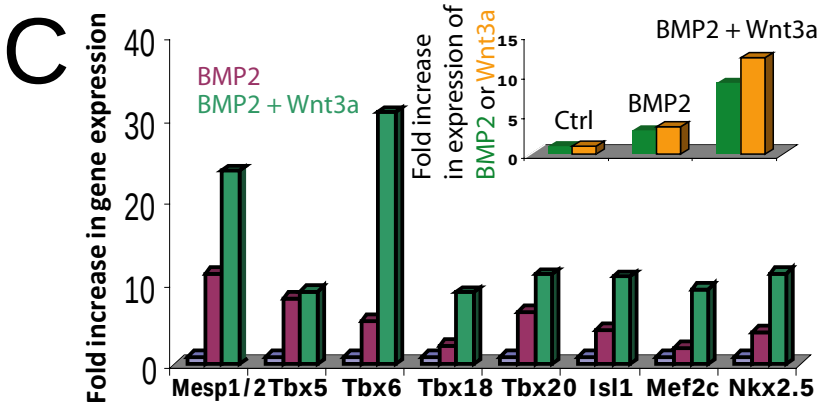

BMP2
OCT4-IA
Basal level
SOX2
OCT4-IA
High level
SOX17
HEX
MESP2
MEF2C
NKX2.5
PLURIPOTENT ES CELLS
ENDO/MESENDODERM
CARDIAC MESODERM
CARDIAC PROGENITOR
Wnt3a
OCT4-IA
SOX2
OCT-SOX
enhancers
Pluripotency gene activation
OCT4-IA
SOX17
pSOX17
HEX activation

Figure 5

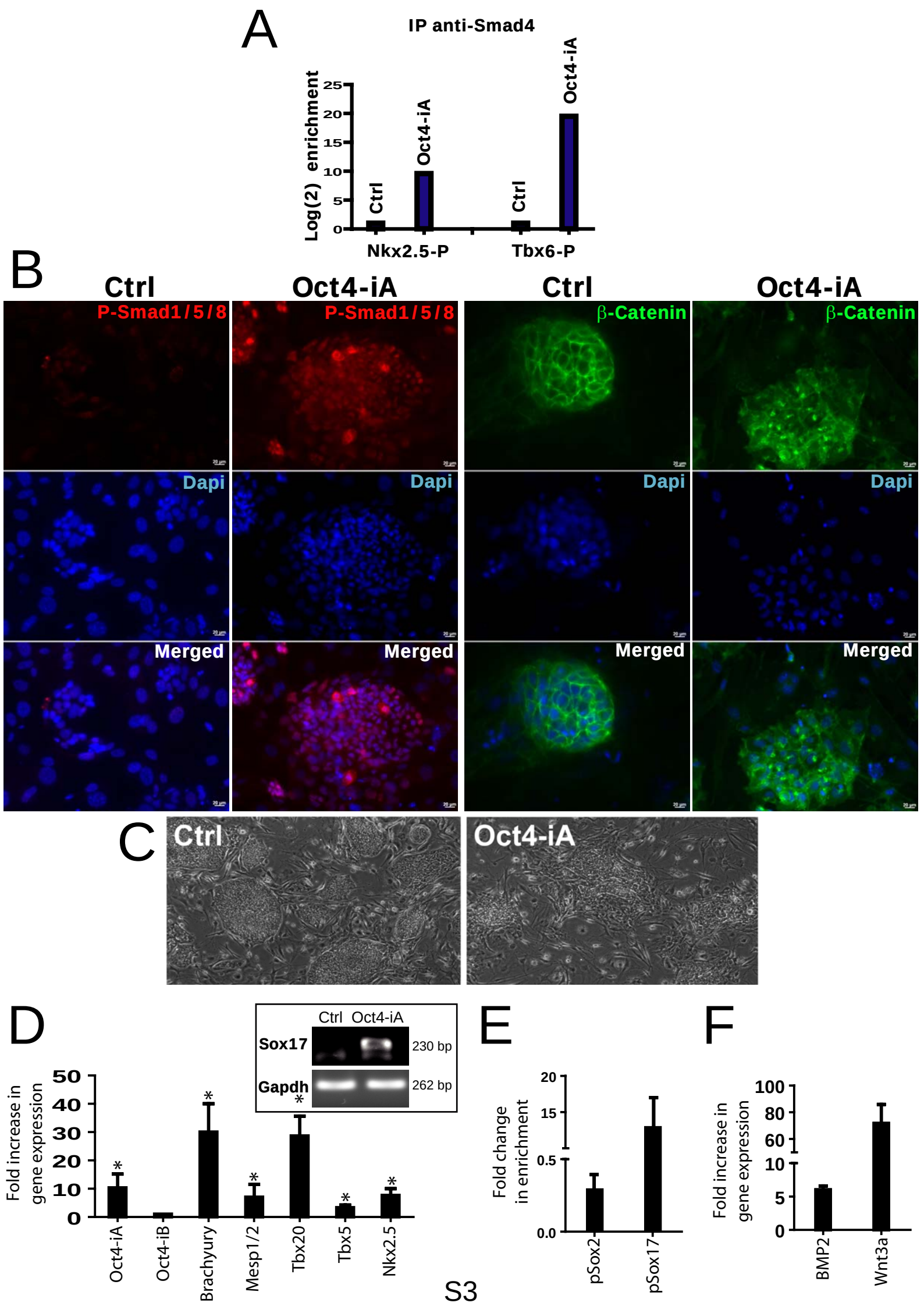

A
HUES-9 pOct4/GFP
GFP
GFP
+COUP-TF1
GFP
+COUP-TF1
B
HUES-9 pOct4/GFP
Fold increase in GFP expression
20000
15000
10000
5000
0
Ctrl
+Oct4-iA
C
CD31
CD34
CD45
Ctrl
Oct4-iA
FL2-Height
R2
CD31
CD34
CD45
12%
1%
1%
D
Fold increase in Sox2 mRNA expression
Ctrl
ShSox2
Sox2
E
Ctrl
ShSox2
34kD
anti-Sox2
F
Ctrl
Oct4-iA
+ ShSox17
Oct4-iA
48kD
anti-Oct4
44kD
anti-Sox17
50kD
anti-Tubulin
G
Fold increase in gene expression
BMP2
BMP2
+ ShSox17
Brachyury
Mesp1/2
Tbx20
Tbx6
Tbx5
Mef2c
Ctrl
BMP2
BMP2 + ShSox17
Sox17
230 bp
Gapdh
262 bp


A
Tbx6
Fold increase in gene expression
8,0
6,0
4,0
2,0
0,0
0:1
1:1
3:1
9:1
Mesp1
10,0
8,0
6,0
4,0
2,0
0,0
0:1
1:1
3:1
9:1
Isl1
15,0
10,0
5,0
0,0
0:1
1:1
3:1
9:1
Tbx5
10,0
8,0
6,0
4,0
2,0
0,0
0:1
1:1
3:1
9:1
Nkx2.5
40,0
30,0
20,0
10,0
0,0
0:1
1:1
3:1
9:1


B
Dapi
GFP
Nkx2.5
3:1
9:1
0:1


C
Fold increase in gene expression
40
30
20
10
0
BMP2
BMP2 + Wnt3a
Fold increase in expression of BMP2 or Wnt3a
15
10
5
0
Ctrl
BMP2
BMP2 + Wnt3a
Mesp1/2
Tbx5
Tbx6
Tbx18
Tbx20
Isl1
Mef2c
Nkx2.5

S2


A
IP anti-Smad4
Log(2) enrichment
25
20
15
10
5
0
Ctrl
Oct4-iA
Ctrl
Oct4-iA
Nkx2.5-P
Tbx6-P
B
Ctrl
Oct4-iA
Ctrl
Oct4-iA
P-Smad1/5/8
P-Smad1/5/8
β-Catenin
β-Catenin
Dapi
Dapi
Dapi
Dapi
Merged
Merged
Merged
Merged
C
Ctrl
Oct4-iA
D
Ctrl Oct4-iA
Sox17
230 bp
Gapdh
262 bp
Fold increase in gene expression
50
40
30
20
10
0
Oct4-iA
Oct4-iB
Brachyury
Mesp1/2
Tbx20
Tbx5
Nkx2.5
E
Fold change in enrichment
20
15
0.5
0.0
pSox2
pSox17
F
Fold increase in gene expression
100
80
60
10
5
0
BMP2
Wnt3a

S3